

A COMPARISON OF THE ATLAS/HERCULES THERMOPHYSICAL ANOMALY AND RADAR-DARK HALO CRATERS. J. T. S. Cahill¹, A. C. Martin¹, G. W. Patterson¹, and S. S. Bhiravarasu². ¹Johns Hopkins University Applied Physics Laboratory, Laurel, MD (Joshua.Cahill@jhuapl.edu), and ²Space Applications Centre (ISRO), Ahmedabad, Gujarat, India.

Introduction: A new class of enigmatic deposits on the Moon has emerged since the Lunar Reconnaissance Orbiter (LRO) entered orbit that contrasts with the lunar regolith at large. Unlike optical anomalies, such as swirls, these deposits are unusual for their thermophysical characteristics. One ubiquitous class consists of lunar cold-spot craters, so-named because they are characterized by extensive regions, relative to their cavity diameter and depth, of anomalously cold regolith temperatures in nighttime Diviner data [2]. These cold regions are not easily explained by conventional impact mechanics. Hayne et al. [1] further characterized these features with high Diviner-derived H-parameter values which provides a convention for describing thermophysical depth profiles. The H-parameter governs the variation of density and conductivity of the lunar regolith with depth and is independent of temperature. The high H-parameter values of cold-spot craters show suggests their thermophysical properties are consistent with a ‘fluffed up’ regolith in the upper 10 to 30 cm created by some aspect of the impact process.

Also reported by [1] were thermophysically distinct signatures associated with pyroclastic flows and a thermophysically unique region near $\sim 45^\circ\text{N}$, $\sim 45^\circ\text{E}$. This region is southeast of Mare Frigoris and is far more expansive than typical cold spots, encompassing the craters Atlas, Hercules, Burg, and Keldysh. With thermophysical similarities to cold spots, initially the region seemed to fit the definition of a cold spot. However, the region is without similar geomorphological characteristics and bears dramatic differences in spatial scale to cold spots and conventional lunar pyroclastic deposits. The ‘Atlas thermophysical anomaly’, as we denote it here, also consists of high H-parameter values relative to its surroundings, suggesting it consists of finer regolith materials, with higher porosities, and with lower thermal inertias than typical regolith. But, the mechanism necessary to form such a large thermophysically distinct region is less clear making it enigmatic even relative to cold-spots. Not only is this region unique, but until recently it was in proximity of two CLPS landing sites; ispace is scheduled to land at Atlas in spring 2023.

As mentioned previously, the regions thermophysical values are consistent with pyroclastic deposits. Further, Atlas crater itself is a floor fractured crater with previously documented evidence of magmatic/volcanic activity in the form of pyroclastic deposits [3, 4]. However, these pyroclastic deposits are localized to the Atlas crater cavity floor and no known studies have inferred

additional expansive volcanic activity that would be coincident with the thermophysical boundaries.

Making the region even more scientifically intriguing, the craters Atlas, Hercules, and Burg have each previously been identified as radar dark halo craters [5]. Ghent et al. [6]’s most recent analysis of the physical properties of radar dark halo craters reported that the halo material is depleted in surface rocks, but are otherwise thermophysically indistinct from background regolith. This contrasts with what we observe in H-parameter maps of the Atlas region. Here, with additional

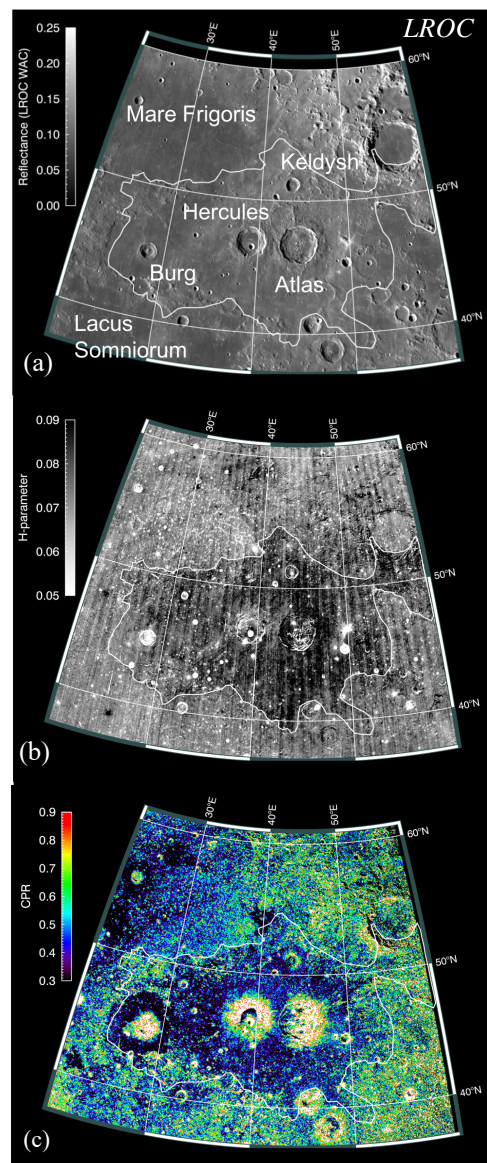


Figure 1: Atlas crater region in (a) LROC WAC, (b) Diviner H-parameter, and (c) AO 70.3 cm CPR radar.

radar, TIR, and gravity data sets for perspective we re-examine the region relative to other traditional radar dark halo craters in search of similarities and differences in formation mechanism(s) and timing.

Objectives: The Atlas region may provide a unique insight into how the lunar regolith is being weathered that contrasts with cold spots in general. For example, unlike the Atlas region, cold spots are not typically detected in radar wavelengths. Here we focus our investigation on the physical properties of the Atlas region and how they may or may not be synergistic with its thermophysical properties with increasing depth. We do this with a combination of monostatic and bistatic radar observations of the region at multiple wavelengths, and we postulate potential formation mechanisms of this region relative to lunar cold spots and radar-dark halo craters (e.g., new craters, pyroclastic deposits, etc.). And finally, we examine GRAIL gravity data to determine if additional information can be derived from the deeper subsurface regarding magmatic/volcanic potential. Questions we aim to answer include: How does the mechanism that formed the Atlas thermophysical anomaly contrast with that of typical cold spots, pyroclastic deposits, and radar dark halo craters?

Methods: Study of this region starts with the analysis of Diviner H-parameter and rock abundance maps relative to Mini-RF monostatic S-band (12.6 cm) and Earth-based Arecibo Observatory-Greenbank Observatory (AO/GO) bistatic P-band (70.3 cm) observations. The contrast in physical sensitivity between circular polarization ratio of these two radar data sets and Diviner's thermophysical information is complementary regarding surface and subsurface material, size, and relative stratigraphic depths. We also compare these data with GRAIL gravity maps to examine the potential for magmatic sources that may have influenced the region.

Arecibo-Mini-RF bistatic observations are also utilized, but targeted at Atlas (due to recent interest with CLPS) and the thermophysical boundaries of the region. The transmitters for Mini-RF bistatic observations are AO (S-band) and DSS-13 (X-band). For each of these observations, the lunar surface is illuminated with a circularly polarized, chirped signal that tracks the Mini-RF antenna boresight intercept on the surface of the Moon. The Mini-RF receiver operates continuously and separately receives the horizontal and vertical polarization components of the signal backscattered from the lunar surface. The resolution of the data is ~ 100 m in range and ~ 2.5 m in azimuth but can vary from one observation to another, as a function of the viewing geometry. The data are coherently averaged onto grids with a spacing of 4 m along track and 20 m cross track. For analysis, they are then incoherently reduced to a uniform 100 m grid yielding approximately a 25-look average for

each sampled location. This also enables a modest improvement in along-track resolution.

Discussions and Observations: In 12.6 and 70 cm image data (Figure 1), the Atlas region shows distinctive low backscatter characteristics more consistent with radar-dark halo craters than lunar cold-spots which are usually undetectable at radar wavelengths [1, 5]. The radar-dark halo craters Burg, Atlas, and Hercules show backscatter properties consistent with lunar regolith devoid of scatterers (boulders, fractures, and corner reflectors) to at least ~ 10 m depths, significantly greater depths than sensed by Diviner. However, Atlas is thermophysically distinct from its surroundings, unlike most radar-dark halo craters which show little contrast in the H-parameter relative to background regolith (Fig. 2), consistent with Ghent et al. [6]'s findings. This suggests something about this region is unique from most other radar-dark halo craters. GRAIL gravity data show a positive Bouguer anomaly running southwest of Hercules and east of Burg which is most likely associated with Mare Frigoris to northeast. While proximity suggests a relationship between the Bouguer anomaly and the Atlas region there is currently no evidence for this. Additional L-band observations of the region with Chandrayaan-2's DFSAR could provide valuable complementary observations for this study.

References: [1] Hayne et al. (2017) JGR, 122, 2371. [2] Bandfield et al. (2014) Icarus, 231, 221. [3] Gaddis et al. (2003) Icarus, 161, 262. [4] Gaddis et al. (2000) JGR, 105, 4245. [5] Ghent et al. (2005) JGR, 110, doi:10.1029/2004JE002366. [6] Ghent et al. (2015) Icarus, doi:10.1016/j.icarus.2015.12.014.

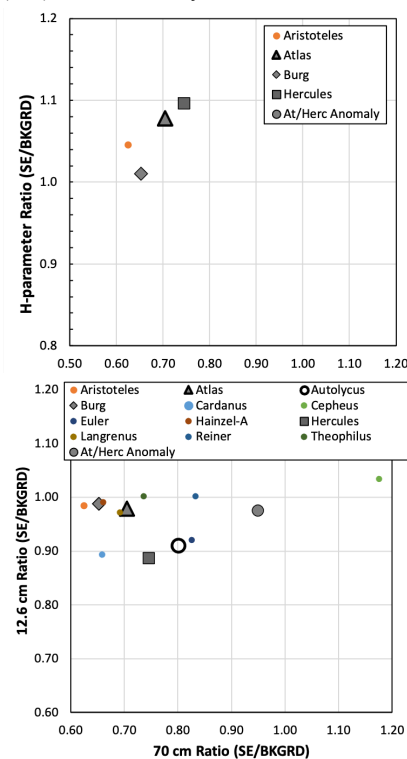


Figure 2: Initial CPR (AO & Mini-RF) and H-parameter measures of secondary ejecta / background regolith.